

BEAM INDUCED FLUORESCENCE MONITOR & IMAGING SPECTROGRAPHY OF DIFFERENT WORKING GASES*

F. Becker[†], C. Andre, P. Forck, R. Haseitl, A. Hug, B. Walasek-Hoehne, GSI, Darmstadt, Germany, F. Bieniosek, P.A. Ni, LBNL, Berkeley, California, D.H.H. Hoffmann, TUD, Darmstadt, Germany

Abstract

Beam induced fluorescence spectra in the range of 300-800 nm were investigated with an imaging spectrograph. Wavelength-selective beam profiles were obtained for a 5.16 MeV/u sulphur beam in nitrogen, xenon, krypton, argon and helium at 10^{-3} mbar gas pressure. In this paper calibrated BIF spectra of specific gas transitions were identified and corresponding beam profiles presented. The measurement results are discussed for typical applications at the present setup and the future FAIR facility.

MOTIVATION

As conventional intercepting diagnostics will not withstand high intensity ion beams, **Beam Induced Fluorescence (BIF)** profile monitors constitute a pre-eminent alternative for online profile measurements [1]. At present, two BIF monitors are installed at the GSI UNILAC and several locations are planned for the FAIR high energy beam transport lines [2]. For further optimizations accuracy issues like gas dynamics have to be investigated systematically. Especially the determination of focused beams in front of targets with high line charge densities rely on a careful selection of proper working gas transitions to keep profile distortions as low as possible [3].

EXPERIMENTAL SETUP

Key issue of this experimental layout using an imaging spectrograph with an area scan intensified CCD (ICCD) camera (Fig. 1) was to have both, the spectral information of specific beam induced gas transitions along the diffraction axis and the spatial information about the beam profile width, transition wise along the imaging axis, see Fig. 2. For 150 mm object distance, a chromatically corrected UV-lens of $f=50\text{mm}$ and $f/2.8$ was chosen. A CCD height of 4.9 mm and a total reproduction scale $\beta_{tot}=0.42$ yield a 19.5 mm field of view.

Imaging Spectrograph & Gas Composition

The $\varnothing 70$ mm spherical mirror with 140 mm focal length is holographically etched and astigmatism corrected. 140 sinusoidal grooves per mm produce a spectral dispersion of 50 nm/mm and an image field of 8×12 mm on the vertical imaging axis and the horizontal dispersive axis, respec-

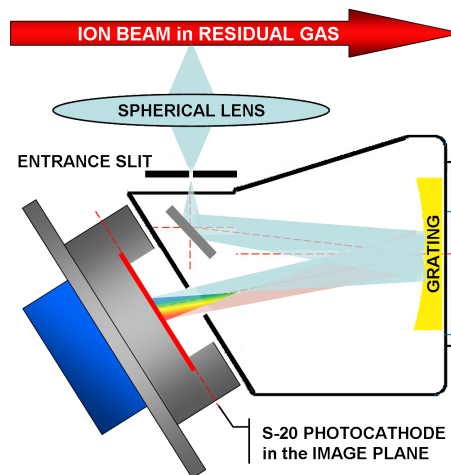


Figure 1: Top-view of the optical path in the diffractive plane. Length of spectrum in the image plane is 10 mm. 1:1 imaging from slit to image plane. All refractive optics adapted to UV-VIS [5]. ICCD performs single photon detection and has a $\varnothing 25$ mm UV-enhanced photocathode with a V-stack MCP [6] and digital VGA camera [7] (bluish).

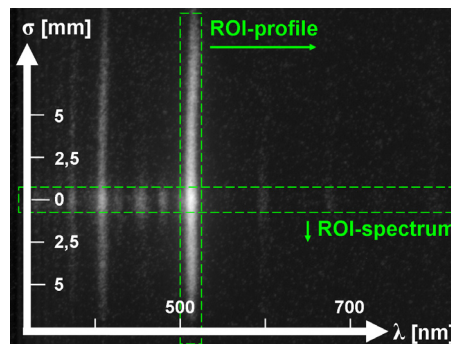


Figure 2: Spectrographic average image $n=2000$ of $3 \cdot 10^{11}$ S^{6+} ions @ MeV/u in 10^{-3} mbar helium gas, $\sigma_w=1.8\text{mm}$. Logarithmic gray-scale for better presentation.

tively. With an optical resolution of 33 lp/mm the ICCD limits the spectral resolution to 1.5 nm for an entrance slit $\leq 30 \mu\text{m}$. The total spectral system efficiency includes all single component efficiencies as a convolution, see Fig. 3 (upper plot). Most limiting factors in the wavelength range ≥ 600 nm are the tri-alkali (Na_2KSb)Cs photocathode and the decreasing grating efficiency. Investigation of optical gas spectra relies on a sufficient purity of the actual gas species. In order to measure and control impurities, a resid-

* Work supported by EU, project FP6-CARE-HIPPI

[†] Frank.Becker@gsi.de

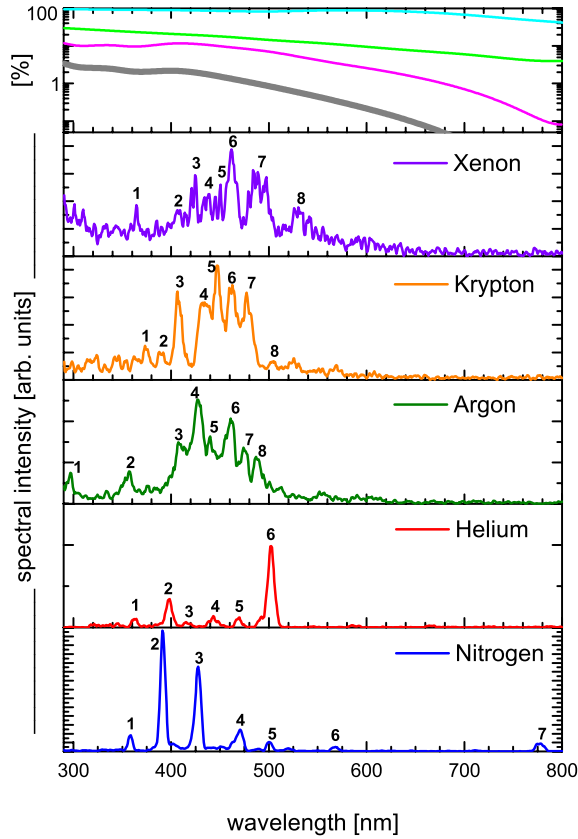


Figure 3: Optical Beam Induced Fluorescence spectra of $3 \cdot 10^{11} \text{ S}^{6+}$ ions @ 5.16 MeV/u in 10^{-3} mbar residual gases (Xe, Kr, Ar, He, N_2). Most prominent transitions are indicated and described in Table 1. Spectral efficiencies (upper plot) in descending order: lens (blue), grating (green), photocathode (magenta) and total (gray).

ual gas analyzer (RGA) 'quadrupole mass spectrometer'-type was used [8]. Base pressure of the unbaked vacuum system was 10^{-7} mbar, with the typical fingerprint of hydrogen, water, nitrogen and traces of the previously introduced rare gas species like krypton in an argon atmosphere. Although the gas leak system was flushed carefully after each gas exchange, a significant source of residuals was the pressure reducing regulator. In order to keep relative impurities below 5 %, the working pressure for all experiments had to be set to 10^{-3} mbar N_2 -equivalent. For set pressures, a gas leak system controls a motorized needle valve so that gas flow rate versus the pump rate allows a dynamic equilibrium. To overcome gas specific variations, the ion gauge (5 % reproducibility) was cross-calibrated to a linear temperature corrected capacitance gauge (0.2 % accuracy), so that the relative error in gas pressure p_{eff} was ≤ 6 %.

DATA ANALYSIS - RESULTS

All optical spectra were recorded during 2000 beam pulses for unchanged accelerator settings. Each single image was recorded as 8-bit bitmap, with the ICCD in photon

05 Beam Profile and Optical Monitors

Table 1: Residual gases (block-wise), observed charge states, observed integral intensity I , I_{gas} normalized to p_{eff} and $I_{gas\&Z}$ normalized to p_{eff} and the e^- -density (upper block line). Corresponding transitions as indicated in Fig. 3, central wavelength and relative intensity with respect to the integral intensity (lower block line). Peaks indicated with No.)^{*} are superpositions of several transition lines.

gas species	charge state	$\sum I$; I_{gas} ; $I_{gas\&Z}$ [%]
Xenon		
	Xe^+/Xe	41; 86; 22
1) 363, 4; 2) [*] 407, 4; 3) [*] 424, 6; 4) [*] 438, 5		
5) 450, 2; 6) [*] 462, 12; 7) [*] 484, 16; 8) [*] 530, 5		
Krypton		
	Kr^+/Kr	45; 63; 25
1) 373, 4; 2) [*] 388, 3; 3) 407, 10; 4) [*] 434, 14		
5) 447, 12; 6) [*] 463, 12; 7) [*] 477, 13; 8) [*] 505, 2		
Argon		
	Ar^+	50; 38; 30
1) 297, 3; 2) [*] 357, 5; 3) [*] 407, 11; 4) 427, 19		
5) [*] 440, 8; 6) [*] 461, 15; 7) [*] 474, 8; 8) [*] 487, 7		
Helium		
	He	21; 4; 26
1) 364, 4; 2) 398, 16; 3) [*] 415, 3; 4) [*] 443, 7		
5) [*] 470, 5; 6) 502, 48		
Nitrogen		
	N_2^+/N^+	100; 100; 100
1) 358, 4; 2) [*] 391, 45; 3) [*] 428, 29; 4) [*] 470, 9		
5) 501, 3; 6) 560, 1; 7) [*] 776, 3		

counting mode. To maintain the dynamic range, the average images were 32-bit float tiffs, see Fig. 2. Further resolution improvement by a factor of ~ 4 was achieved with a cognitive algorithm that determined barycenters of single photon spots and added them as single counts to the VGA-sized matrix [9]. To discriminate spectral peaks against spiky shot noise, Savitzky-Golay fits were applied. Regions of interest (ROI) were chosen like 10 pixel or 40 μm at the beam center for the BIF-spectra in Fig. 3 and like 20 pixel or 16 nm for the transitions specific profile plots in Fig. 4 (mid & bottom).

BIF-Spectra

All spectra were first calibrated to a Hg-Ar-standard and then refined step by step with known transitions of the recorded BIF-spectra. The accuracy for central wavelength is ≤ 1 nm. The investigation was performed with 5 ms long beam pulses of $3 \cdot 10^{11} \text{ S}^{6+}$ ions at 5.16 MeV/u, focused to a σ_w of 1.8 mm. Obtained BIF spectra are depicted in Fig. 3. They were not normalized to the spectral efficiency of the optical components, which is therefore given in Fig. 3 as well. In Table 1, the observed charge states, relative integral intensities and most prominent transitions are listed. Different signal-to-noise ratios for the gas species are determined by the observed integral intensity I . Beside nitrogen and helium, where spectral lines of optical transitions are separated, lines appear less intense and clustered in groups. Although nitrogen shows the brightest transi-

tions, gases like xenon and krypton show similar integral intensities I_{gas} , normalized with respect to p_{eff} . To account for the electronic stopping power, integral intensities $I_{gas&Z}$ have been furthermore normalized to the electron-density $\propto Z$. This way, all rare gases show similar relative integral intensities, except for nitrogen having a four times higher integral intensity value. When the ROI was moved from the center to the beam fringes, spectral intensity decreased homogeneously for all gases unlike helium which showed an unequal decrease for different transitions. For proton beams as well as for much heavier Ta beams, similar results were obtained. A more detailed description can be found in [10].

Transition Dependent Profile Data

The spectrally resolved profile plots are presented in Fig. 4. In the upper plot, all gas-species show corresponding profile width, besides helium that shows a factor 2.5 larger σ_w . Transition-wise profile data is shown in Fig. 4 for N_2 (middle) and He (bottom). In the case of nitrogen, the transitions 1), 5) and 6) show a slightly increased profile width that can be explained by an upscaling of noise in the profile fringes due to the normalization to a common maximum. He-profile contributions by 1) and 6) show significant shoulders but 2) and 3) do not. Since both He-cases contain weak and strong contributions, noise scaling effects do not explain these results. Assuming excited states of He 1), 2) might have large cross-sections for electron excitation, an 8 mm halo is reasonable, as the mean free path of secondary electrons is in the order of 10 mm, for $p_{eff}=4 \cdot 10^{-3}$ mbar.

CONCLUSION

As first experimental outcome, optical spectra of nitrogen, xenon, krypton, argon and helium have been successfully recorded. They excellently agree with measurements at lower energies ≤ 10 MeV/u in the case of nitrogen [11, 12] and higher energies in the range of 50 MeV/u to 25 GeV/u for nitrogen and xenon [13]. Nitrogen seems to be the most appropriate residual gas, because of its spectral concentration between 390 and 430 nm. In addition, nitrogen shows the highest integral intensities. Especially the four times higher $I_{gas&Z}$ makes it the right choice, if the stopping power is an issue. For electric fields in the order of 10 kV/mm the trajectories of excited, charged molecules like N_2^+ , will be influenced by the beam's space charge and might falsify the profile reading [14]. Therefore one might focus on different selection criteria as larger molecule masses and shorter transition-lifetimes, provided by rare gases like Xe and Kr. Helium is no alternative due to its wrong profile image in the considered pressure range. However, for most beam parameters N_2 is the optimal choice because of its high light yield. Moreover it was shown that all nitrogen profiles show the same profile width. Once a residual gas is selected, optical components can be further optimized.

05 Beam Profile and Optical Monitors

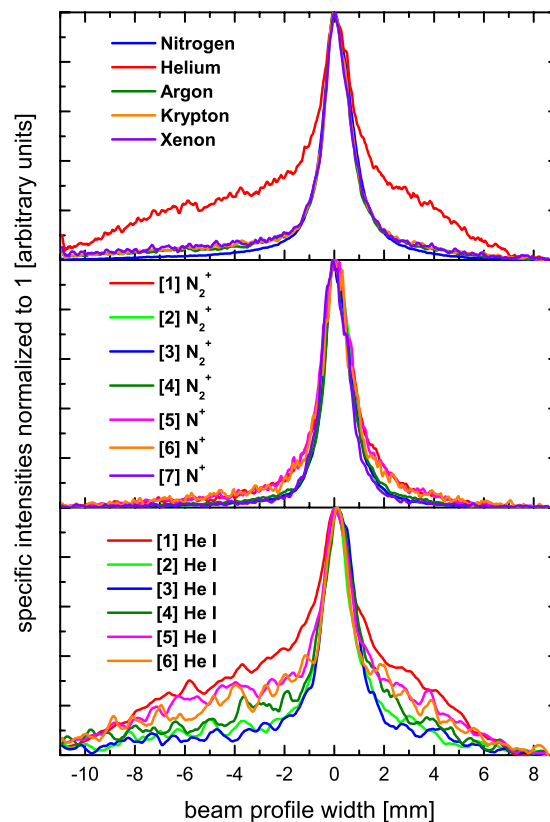


Figure 4: Gas specific beam profiles (upper plot) and transition specific beam profiles for nitrogen (middle) and helium (bottom) as indicated in Fig. 3.

REFERENCES

- [1] P. Forck et al., DIPAC'05, ITTA01, p. 223-227, 2005.
- [2] M. Schwickert et al., DIPAC'09 WEOA04, 2009 & FAIR Baseline Technical Report, Vol. 2, p. 148-162, 2006.
- [3] F. Becker et al., DIPAC'07, MOO3A02, p. 33-36, 2007.
- [4] company: www.horiba.com, CP140-202 140mm Imaging Spectrograph.
- [5] company: www.linor.com, inspec.x 2.8/50 UV-VIS apochromatically corrected lens system.
- [6] company: www.proxitronic.de, BV 2581 QY-V 100N.
- [7] company: www.baslerweb.com, Type 311-f VGA Sony ICX414AL Sensor.
- [8] company: www.pfeiffer-vacuum.de, Gauge PKR-261, Valve EVR-116, Controller RVC-300, Calibration-Gauge CMR-264, RGA PrismaPlus.
- [9] software: <http://rsbweb.nih.gov/ij/>, Img. proc.
- [10] F. Becker, "Non-destructive Beam Profile Measurement of high intense HI-Beams", PhD-thesis, Darmstadt, 2009.
- [11] R.H. Hughes et al., Phys. Rev., **123**, 2084 (1961)
- [12] C. S. Lee et al., "Study of N_2^+ first negative system" Nucl. Instrum. Meth. **B 140**, p. 273-280, 1998.
- [13] M. A. Plum et al., "N2 and Xe gas scintillation @ Cern PS and Booster", Nucl. Instrum. Meth. **A 492**, p. 74-91, 2002.
- [14] F.Becker et al., BIW'08, California, TUPTPF054, 2008.